Low-Temperature Cyclic Voltammetry. 2.[1] Conformational Analysis of Cyclic Tetraalkylhydrazines

Stephen F. Nelsen,* Luis Echegoyen, Edward L. Clennan, Dennis H. Evans,* and Dennis A. Corrigan

Contribution from the Department of Chemistry, University of Wisconsin, Madison, Wisconsin 53706. *Received August 9, 1976*

Abstract: Cyclic voltammograms for 1,2,3-trimethylhexahydropyridazine (**1**), 1,2-dimethyl-1,2,3,6-tetrahydropyridazine (**2**), *cis*-1,2,3,6-tetramethylhexahydropyridazine (**3**), and 1,2-diethylhexahydropyridazine (**4**) all show the appearence of a second, irreversible oxidation peak at low temperature, which grows in size relative to the first peak as the scan rate is increased and ultimately becomes far larger than the first peak. For 1,2-dimethylhexahydropyridazine (**5**) the first peak always remains larger than the second, and no second peak was observed for 1,5-diazabicyclo[4.4.0]decane (**6**) or 1,5-diazabicyclo[4.3.0]nonane (**7**). It is proposed that diequatorial *N*-alkyl (H_{ee}) conformations are responsible for the first peak at low temperature and axial,equatorial (H_{ae}) conformations for the second. Digital simulations assuming that the oxidation of H_{ee} conformations are nearly reversible (rapid), but that the H_{ae} oxidations are irreversible (slow), show good fit to the observed curves. Values of $([H_{ee}]/[H_{ae}])\sqrt{k_t}$ (where k_t is the sum of the first-order rate constants for $H_{ee} \rightarrow H_{ae}$ and $H_{ae} \rightarrow H_{ee}$) obtained from the simulations are consistent with experimental data obtained by ^{13}C NMR and photoelectron spectroscopy.

A variety of tetraalkylhydrazines show electrochemically reversible (or nearly reversible) oxidation at room temperature, and we have reported slow scan cyclic voltammetry (CV) studies of several examples. In a communication[1] we reported that, at low temperatures, some cyclic hydrazines containing hexahydro- and tetrahydropyridazine structures exhibit two oxidation peaks, but only one reduction peak. We have now analyzed these curves using digital simulations and describe how low-temperature cyclic voltammetry may be used as a tool for conformational analysis of these compounds.

Qualitative Considerations

A description of the appearance of the CV curves obtained for 1,2,3-trimethylhexahydropyridazine (**1**) illustrates the

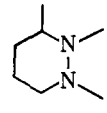

1

phenomenon. Although this compound shows an ordinary CV curve at room temperature, different behavior is exhibited at −55 °C (using butyronitrile as solvent[3]). As shown in Figure 1, at a 50 mV/s sweep rate, some extra current is observed at higher potential than the room-temperature oxidation peak. As the sweep rate is increased, a second oxidation peak, which moves progressively to higher potential, and grows in size relative to the first peak, is observed. These effects were completely physically reversible, the second peak disappearing when the temperature was raised and reappearing again upon lowering the temperature. Qualitatively similar behavior was displayed at a platinum electrode and also in other solvents (acetone, methylene chloride).

Other compounds which showed the second oxidation peak much larger than the first at low temperature and fast scan rate were **2–4.** Quite low temperature (−70 °C) was required to see the appearance of a second oxidation peak for **5,** and the first peak remained larger than the second, in contrast to **1–4.** For **6** and **7,** no trace of a second oxidation process was seen under any conditions.

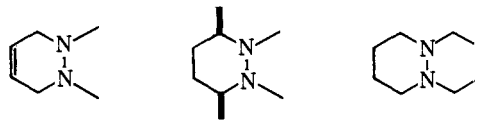

2 **3** **4**

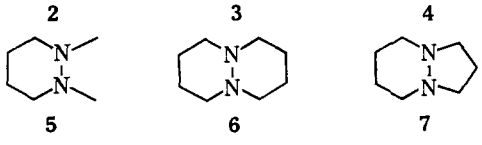

5 **6** **7**

As previously proposed,[1] the observation of a second oxidizable species only at low temperature and faster scan rates seemed to indicate that separate oxidation peaks were being observed for different conformations of these compounds. *N,N'*-Dialkylhexahydropyridazines have two different types of conformations separated by rather high (about 10 kcal/mol) activation barriers, exemplified by those with diequatorial *N*-alkyl groups (which we will designate as H_{ee}) and those with axial,equatorial *N*-alkyl groups (H_{ae}), shown for **5** below.

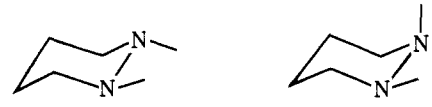

H_{ee} H_{ae}

When the equilibrium between these conformations becomes slow compared with the sweep rate, different oxidation peaks would be observed for oxidation of H_{ee} and H_{ae} if their peak potentials were sufficiently different.

The techniques of low-temperature ^{13}C NMR[4] and photoelectron spectroscopy[5] have been used to establish the conformational preferences for **1–7.** For **1–4,** the ae conformation predominates at equilibrium, while the ee conformation is slightly preferred for **4** and only the ee conformation is populated for **6** and **7.** These preferences fit the observed relative sizes of the first and second oxidation peaks at low temperatures and fast scan rates if it is assumed that the first peak corresponds to oxidation of H_{ee} and the second, that of H_{ae}.

Only one wave for reduction of $H\cdot^+$ to the neutral hydrazine was observed for any compound. This is not surprising on the basis of our conformational argument, because ESR work[6] has shown that the conformations of hydrazine radical cations are quite different from those of the neutral hydrazines. The radical cations are considerably (but not quite completely) flattened at nitrogen, and there is a strong restoring force toward having the lone pair orbitals coplanar. Activation energies for double nitrogen inversion in the radical cations are quite low,[6] and one would expect that these cations would rapidly interconvert between available conformations at accessible temperatures. From the fact that $Ep^{ox\text{-}2}$ (the peak potential for the second oxidation wave) moves to higher potential considerably more rapidly than does $Ep^{ox\text{-}1}$ as the sweep

rate is increased, it is clear that electron transfer from H_{ae} is slower than that from H_{ee}. The electron transfer giving rise to the second wave is slow and appears electrochemically irreversible. In contrast, the wave for H_{ee} oxidation appears nearly electrochemically reversible. It seems likely to us that the large difference in lone pair–lone pair dihedral angle, about 60° for H_{ae}, but about 180° for H_{ee}, such that the lone pairs are approximately coplanar, as is required in the cation radical, is responsible for the difference in rates of electron transfer.

The mimimal kinetic scheme that arises from the above considerations is that shown in Scheme I, in which k(ee → ae)

Scheme I

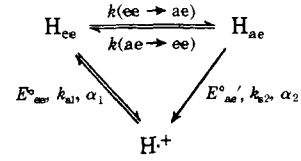

and k(ae → ee) are first-order rate constants, and $E°$, k_s, and α are the standard potential, standard heterogeneous electron-transfer rate constant, and electron-transfer coefficient for the respective electrode reactions.

Generation of Theoretical Votammograms by Digital Simulation

To test whether the observed spectra would actually correspond to the above simple scheme, in which the conformational interconversion between H_{ee} and H_{ae} is completely unaffected by the presence of the electrode, a method of generating the CV curves which would result if Scheme I operated, is clearly required.

Theory for cyclic voltammetry for this CEE reaction scheme was developed by Shuman and Shain[7] who restricted their treatment to the case of reversible electron transfer for the first peak. The digital simulation technique[8] modified by using the steady-state approximation[9] was chosen for the present work because of the ease with which electron-transfer kinetics (quasireversibility) can be introduced into the model.

Though Ruzic and Feldberg[9] demonstrated that their "heterogeneous equivalent" approach gave accurate simulations for the CE mechanism for chronoamperometry, and one of us[10] has shown that equally satisfactory results are obtained for the EC and EC_{dimer} mechanisms for cyclic voltammetry, it was deemed necessary to check the veracity of the approach for the CE process for cyclic voltammetry.

This was done by comparing results of the digital simulations using the "heterogeneous equivalent" approach[9] (our computer program will be provided upon request) with the results for the CE case obtained by the well-established integral equation procedure.[11,12] Specifically, the digital simulations were performed using a total of 2080 time units for the entire cycle. The values of the current function so obtained were within ±0.001 (average deviations; largest deviation was 0.009) of the earlier results (uncertainty of these is +0.000, −0.002[11]) for values of the kinetic parameter, $\kappa = a^{1/2}/k_t^{1/2}K_{eq}$, ranging from 0 to 100 ($k_t = k_f + k_b$ and $a = nFv/RT$ where v is the scan rate). Thus the procedure produces theoretical voltammograms of sufficient accuracy for comparison with the experimental data.

The steady-state approximation should and does[10] fail when a/k_t becomes very large (e.g., fast experiments and/or small rate constants). In addition, the calculations of Nicholson and Shain[11] are not accurate for large a/k_t due to a restrictive assumption in their numerical integrations. Hence, it seemed possible that the good agreement cited above for values of κ as large as 100 could have resulted from approximately similar failure of both types of calculation. However, direct simulation[8] for $\kappa = 100$ (no steady-state assumption) produced values for the current function agreeing to within 0.001 unit with each of the other approaches. Thus it is concluded that the steady-state approximation gives accurate results for values of the kinetic parameter up to 100. Larger values are not normally of experimental interest.

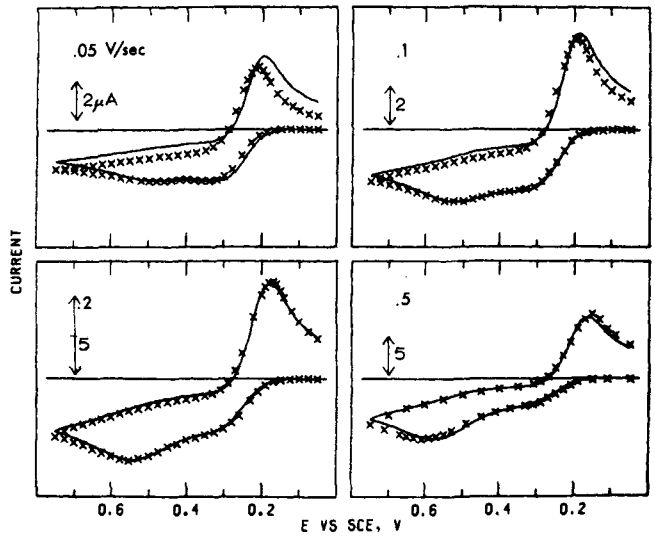

Figure 1. Plots of experimental (X) and calculated (solid line) cyclic voltammograms for **1** at −55 °C, scan rate 50, 100, 200, 500 mV/s. The following parameters were set as constants for these simulations: apparent $E°_{ee} = 0.255$ V, $K_{eq}\sqrt{k_1} = 0.68\ s^{-1}$, $\alpha_1 = 0.5$, $k_{s1}/\sqrt{D} = 20.2\ s^{-1/2}$, $\alpha_2 = 0.7$, $k_{s2}/\sqrt{D} = 4.34 \times 10^{-3}\ s^{-1/2}$, referred to arbitrary $E°_{ae}' = +0.125$ V.

The accuracy of digital simulations for generating cyclic voltammograms with rate-limiting electron transfer has been verified in earlier work.[13]

Comparison of Experimental CV Curves and Digital Simulations

We soon found that a uniform method of electrode surface preparation is critical for obtaining reproducible results. The position of the second oxidation peak is particularly sensitive to all experimental variables. In our recent work, a freshly polished gold electrode is held at −3.0 V vs. SCE for 3 s, and then at +3.0 V for 3 s. This pretreatment is followed by an aging, allowing the electrode to stand at a potential where no current is passed for several minutes. If cyclic voltammograms are run immediately after the electrochemical pretreatment, a second oxidation peak is observed even at room temperature and 100 mV/s scan rates for some compounds, but the position of this second peak drifts toward the first with time, and after a few minutes, only a single, "reversible" oxidation wave is observed. Interestingly, the extra peak has never been observed for **6** and **7**, which exist exclusively in diequatorial conformations. There obviously is much to be learned about the surface of our "gold" electrodes, but pretreatment and aging of the electrode as described above gives reproducible CV curves for many hours with the compounds described here.

Solvent purity is also critical. The curves originally published for **1**[1] have a smaller reduction peak than those obtained more recently (Figure 1). We found that the size of the reduction peak is especially sensitive to the quality of the butyronitrile used and that this peak is consistently larger if the solvent is given a final purification by a careful distillation employing a spinning band column.

Theoretical voltammograms are presented in Figure 1 along with experimental data for four scan rates for the oxidation of 1,2,3-trimethylhexahydropyridazine (**1**). The values of all simulation parameters have been held constant for the simulations shown, which are based upon linear diffusion, with the

diffusion coefficients of all species assumed equal. The shape of the first peak and its dependence upon scan rate are indicative of a CE process,[11] and it is apparent from Figure 1 that the model adequately duplicates this feature. The second peak becomes prominent at the more rapid scan rates, and its height relative to the first peak as well as its shape and position are well simulated by the simple, irreversible oxidation of H_{ae} assumed in Scheme I with $\alpha_2 = 0.7$. The observed currents at potentials positive of the second peak are somewhat greater than the simulated values because of the onset of the oxidation of the radical cation, a process not included in the simulations.

A single reduction peak is found on the return half-cycle. At slow scan rates the observed reduction peak current is less than predicted, which may indicate a slow decomposition of the radical cation. As mentioned above, the reduction peak current was distinctly lower when the solvent had not been distilled through a spinning band column. Better agreement was found when such a decomposition reaction was included in the simulations, but this refinement was not thought to enhance significantly the analysis of the data.

The separation between the first anodic peak and the cathodic peak increased with increasing scan rate, an effect caused by a combination of partially rate-limiting electron transfer and uncompensated solution resistance. The maximum error due to the latter factor is estimated to be about 60 mV by taking the product of the largest current observed (20 μA) and the total cell resistance (3 kΩ at −55 °C) as measured from counter to working electrode. The actual uncompensated resistance will be less than 3 kΩ. The shapes of the first oxidation peak and the reduction peak were simulated by using partially rate-limiting electron transfer both because the resistance effects were small and because the effects of uncompensated resistance and slow electron transfer are extremely similar.[14-16] The two effects were not separated in the present work so the electron-transfer kinetic parameters used in the simulation are of very limited significance, and we shall not attempt interpretation.

Returning to the second oxidation peak, which we attribute to irreversible oxidation of H_{ae}, it is of interest to identify the factors which make possible a large enough separation between the first and second peaks to permit their clear resolution. The first factor is the difference between the standard potentials ($E°_{ae}' - E°_{ee}$). If H_{ae} is oxidized directly to the radical cation, $E°_{ae}'$ only differs from $E°_{ee}$ by the difference in free energy of H_{ae} and H_{ee}. Although the NMR spectrum of **1** is too complex for analysis,[4a] photoelectron spectroscopy has shown that H_{ae} conformations predominate and that at least a few percent of H_{ee} conformations are present in the vapor phase.[5] In all cases where the comparison has been possible, the techniques of ^{13}C NMR and photoelectron spectroscopy have been in excellent agreement for conformational preferences.[4] If there were 5% H_{ee} conformations present at −50 °C, $\Delta G°$ (**lee** − **lae**) would be 1.3 kcal/mol, corresponding to only a 56 mV difference in $E°$, far too small to allow resolution of the two oxidation peaks. The H_{ee} form is 0.3 kcal/mol stabler than the H_{ae} form for **5**, yet we still observe two oxidation peaks. One possibility would be that H_{ae} is oxidized to a cation resembling it in geometry, so that $E°_{ae}'$ is determined not by adiabatic, but by vertical electron removal. Even in this case (which seems unlikely to us) the separation of the peaks observed cannot be caused by $E°$ differences, since our photoelectron spectroscopy work has shown that the vertical ionization potentials differ by under 300 mV.[5]

Thus any difference in standard potentials for H_{ae} and H_{ee} is not sufficient to explain the resolution of the two oxidation peaks. It is necessary that the heterogeneous electron-transfer rate constant for the process occurring at more positive potentials be much less than that for the first process, which causes the second peak to occur increasingly positive of its standard potential as the scan rate increases. As stated above, we suggest that the small heterogeneous electron-transfer rate constants for H_{ae} are connected with the gauche lone-pair geometry of these conformations. In addition, the magnitude of the H_{ae} electron-transfer rate constant is affected by the condition of the electrode surface.

Table I. Kinetic Parameters for **1** from Digital Simulation of the CV Curves

Temp, °C	v, V/s	κ	$K_{eq}\sqrt{k_t}$
−45	0.10	1.90	1.16
−50	0.10	2.50	0.89
−55	0.05	2.34	0.68
−55	0.10	3.31	0.68
−55	0.20	4.60	0.68
−55	0.50	7.41	0.68
−60	0.10	5.00	0.46
−65	0.10	6.50	0.35

Strictly speaking, our simulations show that a CEE mechanism is operative, but they do not indicate the species responsible for the peaks. In view of the basicity of the hydrazines, it might be supposed that the first oxidation peak could be due to oxidation of the free hydrazine, while the second was caused by oxidation of the protonated form, present because of acidic impurities. The CEE scheme (Scheme II) might be argued to be a possibility (B is the hydrazine). The fact

Scheme II

$$BH^+ \underset{k_b}{\overset{k_f}{\rightleftharpoons}} B + H^+$$

$$B \overset{E°_1}{\rightleftharpoons} B^{\cdot+} + e \text{ (reversible)}$$

$$BH^+ \xrightarrow{E°_2'} B^{\cdot+} + H^+ + e \text{ (irreversible)}$$

that voltammograms qualitatively similar to those obtained in butyronitrile were also observed in dichloromethane and acetone argues against Scheme II. Furthermore, even addition of a 50 molar excess of butyric acid to the butyronitrile did not alter the relative peak heights appreciably, as would be required by Scheme II.

Kinetics for Conformational Interconversions by Cyclic Voltammetry

The relatively good fit of the digital simulations to the experimental voltammograms indicates that Scheme I, in which the conformational interchange is independent of the presence of the electrode, may be an adequate description. If this is true, the equilibria and kinetics for the conformational change can be extracted from the digital simulation data.

As discussed above, the electron-transfer kinetic parameters are of very limited significance because of resistance problems at low temperatures. Nevertheless, information about the kinetics of the conformational change could be reasonably accurate. For this purpose, the significant parameter obtained from the digital simulations is the kinetic parameter, $\kappa = a^{1/2}/K_{eq}k_t^{1/2}$, where $a = vnF/RT$, $K_{eq} = [H_{ee}]/[H_{ae}]$, and $k_t = k_{ee\to ae} + k_{ae\to ee}$. This kinetic parameter yields $K_{eq}\sqrt{k_t}$ directly. Table I contains the data for our most intensively studied case, **1**, at several temperatures. The regular change in κ as the temperature is lowered, and reasonable constancy of $K_{eq}\sqrt{k_t}$ at four scan rates at a single temperature (see Figure 1), is gratifying. These electrochemical data do not allow separation of K_{eq} from k_t. The conformational change is so rapid that at all of our temperatures, the relative sizes of

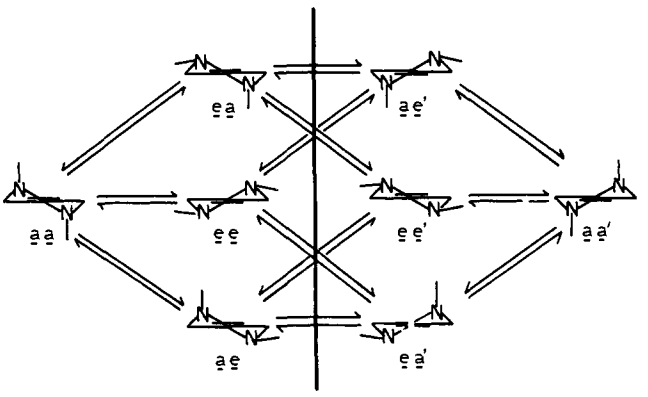

Figure 2. Conformational diagram showing the interconversions between the eight conformations of **2**.

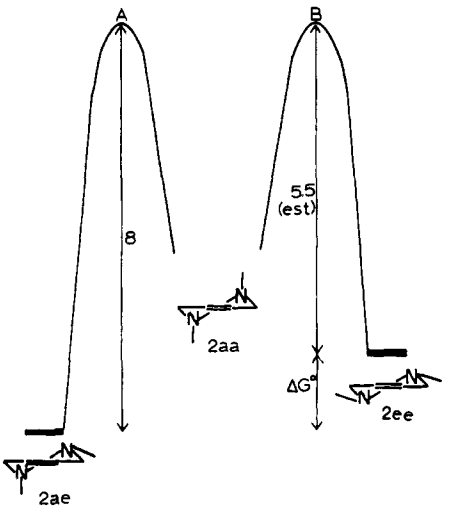

Figure 3. Schematic energy diagram for the interconversion of **2ae** and **2ee.**

oxidation peaks 1 and 2 were still changing with scan rate. In such regions, a significant value for κ can be obtained, but not for K_{eq}.

As mentioned above, the photoelectron spectrum of **1** showed that a few percent of H_{ee} conformations are present at room temperature. From the kinetic parameters given in Table I, if $K_{eq} = [H_{ee}]/[H_{ae}] = 0.11$ (10% H_{ee} at equilibrium), $\Delta G^{\ddagger}$ ($H_{ee} \rightarrow H_{ae}$) = 11.14 kcal/mol (average of the data at the five temperatures studied, -55 ± 10 °C, deviation in calculated values ±0.03); the corresponding numbers for 5 and 15% H_{ee} at equilibrium are 10.47 and 11.56 kcal/mol, respectively. The $\Delta G^{\ddagger}$ ($H_{ee} \rightarrow H_{ae}$) at −55 °C for the dimethylated analogue, **5**, is 10.4 kcal/mol,[4a] determined by NMR (in acetone). The presence of the extra methyl in **1** should not raise the activation energy for the ring flip which is the highest barrier between H_{ee} and H_{ae} more than a couple of tenth's of a kcal/mol, so the agreement of the $\Delta G^{\ddagger}$ calculated from the electrochemical data with that derived from ^{13}C NMR is remarkably good, especially considering the great difference in the types of experiment performed.

Simulation gave a $K_{eq}\sqrt{k_t}$ value of 1.3 at −55 °C for tetrahydropyridazine **2.** Anderson[17] showed that the lowest of the higher energy nitrogen inversion and ring reversal (these which cross the central line of the conformational diagram in Figure 2) is about 12 kcal/mol, considerably higher than that of the lower energy nitrogen inversion, which converts **2ae** to **2aa.** We redetermined the latter barrier by ^{13}C NMR, obtaining a $\Delta G^{\ddagger}$ (−55 °C) of 8.0 kcal/mol.[4b] An energy diagram for conversion of **2ee** to **2ae** is shown in Figure 3. The higher barrier will either be point A [corresponding to a $\Delta G^{\ddagger}$ (**2ee** − **2ae**) of 8 − $\Delta G°$ (**2ee** − **2ae**)] or B, the activation energy for the **2ee** → **2aa** ring reversal. This latter number cannot be directly measured since neither **2ee** nor **2aa** is present in detectable concentration, but we point out that it is probably quite near the 5.4 kcal/mol observed for cyclohexene.[18] The presence of the nitrogens should not appreciably affect the barrier because their lone pairs are nearly perpendicular at the transition state. As an excellent analogy, the lower ring reversal barrier of **5**[4a] is 10.5 kcal/mol (−67 °C), close to the 10.2 (−67 °C) measured for cyclohexane.[19]

The fact that $\Delta G°$ (**2ee** − **2ae**) must be substantial to preclude detection of **2ee** makes it exceedingly likely that point B in Figure 3 is above A, making the lower energy ring reversal the rate-limiting step in **2ee** → **2ae** conversion. Combined with the $K_{eq}\sqrt{k_t}$ value of 1.3, a $\Delta G^{\ddagger}$ (**2ee** → **2ae**) of 5.5 kcal/mol gives a calculated $\Delta G°$ (**2ee** − **2ae**) of 3.4 kcal/mol. Even if $\Delta G^{\ddagger}$ (**2ee** → **2ae**) were higher than the 5.5 kcal/mol estimated, $\Delta G°$ (**2ee** − **2ae**) is still calculated to be large; an activation energy of 7 kcal/mol gives $\Delta G°$ of 2.7 kcal/mol (corresponding to 0.2% **2ee** at −55 °C).

The value of $K_{eq}\sqrt{k_t}$ obtained is entirely consistent with the failure to detect **2ee** and, combined with a reasonable estimate for the lower energy ring reversal barrier, gives a probable $\Delta G°$ (**2ee** − **2ae**) of over 3 kcal/mol.

The $K_{eq}\sqrt{k_t}$ value obtained by simulation of the −29 °C CV of **3** was 0.73. By ^{13}C NMR, interconversion of the mirror image H_{ae} forms, which is likely to proceed through H_{ee} as an intermediate, has $\Delta G^{\ddagger}$ (−29 °C) of 11.8 kcal/mol.[4a] Thus $\Delta G^{\ddagger}$ (**3ee** → **3ae**) might well be 11.8 − $\Delta G°$ (**3ee** − **3ae**). It is also possible that the lowest energy pathway for the conversion would instead involve the ring flip which gives **3aa.** The activation energy for this process in the dimethyl compound **5** is 10 kcal/mol, and the methyl substitution is not expected to change the activation energy much.[4a] Use of a barrier of 10 kcal/mol in combination with the $K_{eq}\sqrt{k_t}$ value gives a $\Delta G°$ (**3ee** − **3ae**) of 2.2 kcal/mol (1% ee at −29 °C), if a lower energy pathway were available, a higher $\Delta G°$ (**3ee** − **3ae**) value would be calculated. Thus the $K_{eq}\sqrt{k_t}$ value observed is consistent with not detecting **3ee.**

Conclusion

Scheme I for these cyclic hydrazines was tested by digital simulation and seems adequate. The most valuable parameter obtained from the simulations is $K_{eq}\sqrt{k_t}$. The values of this parameter obtained for **1**–**3** were quite consistent with known conformational information about these systems, giving us confidence that the electrochemically derived parameter has the physical significance we have attributed to it and that Scheme I really holds.

The rate constants affecting the cyclic voltammogram are significantly different from those affecting the low-temperature NMR spectrum, and when these techniques are used in conjunction, significant information not previously obtainable is gained. For example, $\Delta G°$ (**2ee** − **2ae**) was measured electrochemically to be almost certainly above 3 kcal/mol. Recording the low-temperature NMR of **2** does not allow sufficient confidence that **2ee** is not present in small amount to push $\Delta G°$ nearly as high.

The electrochemical technique separates the conformations into classes of fast and slow oxidation (H_{ee} and H_{ae} for these compounds). This simplification can be important for an unsymmetrical molecule like **1** (which has four different H_{ae} and two different H_{ee} conformations), where the low-temperature NMR spectrum is too complicated to interpret.

In principle, the value for K_{eq} is separately obtainable by the electrochemical technique, since all that must be done to get it is to run the voltammogram at low enough temperature and

fast enough scan rate so that the relative sizes of the two oxidation peaks are no longer dependent on scan rates. Under these conditions, k_t has been "frozen out", and the simulation gives K_{eq} directly. In practice this is not easy for the compounds studied, because even in butyronitrile, we have serious resistance problems below −60 °C, tending to broaden the oxidation peaks and obscure their resolution, and resistance problems also become increasingly great at faster scan rates. We were unable to achieve this condition for **1**, although the observed ratio of peak currents at −60 °C and 5 V/s scan rate was 0.3, so K_{eq} must be less than this value.

For use of cyclic voltammetry as a tool for conformational analysis, a compound must have conformations separated by significant activation barriers, which oxidize or reduce at substantially different rates. Six-membered ring hydrazines obviously meet these requirements, and valuable kinetic information which supplements that from other techniques is available. Whether other classes of compounds will meet both requirements remains to be seen.

Experimental Section

The preparation of the compounds has been previously given;[4] final purification was by VPC immediately before use.

Electrochemistry. A Princeton Applied Research Corp. Model 170 instrument was employed. The cell was of Pyrex construction, the solvent compartment consisting of a 30 mm long cylinder, 23 mm in diameter, fused to the bottom of a 250-ml round-bottomed flask fitted with five 14/20 joints. The solvent compartment is surrounded by a cylindrical cooling jacket 30 mm in diameter by 45 mm long, fitted with gas inlet and outlet protruding through a 57 mm diameter × 50 mm cylindrical evacuated jacket. Temperatures were measured with a Leeds and Northrup 8693-2 potentiometer. The coolant nitrogen was passed through a stainless steel heat exchanger immersed in dry ice, the temperature being changed by changing the flow rate. The temperature inside the cell was measured with the nitrogen bubbler going and remains constant to the ±0.5 °C readability of the thermocouple for many minutes. Temperature gradients undoubtedly develop within the cell when the nitrogen bubbler is turned off to allow a voltammogram to be run, but the same temperature is measured on the thermocouple when the bubbler is turned on again after the run.

The working electrode consists of a 3.0 mm gold rod force fit into a Teflon support tube and mounted coaxially with the cell. After preliminary polishing with fine emery paper (0 to 0/3 grades), the gold electrode was polished using aqueous suspensions of alumina (Fisher Scientific Co.), 3, 1, and 0.1 μm, on a polishing cloth mounted on a wheel. Pretreatment and aging are described in the text. The other four necks of the cell hold the reference electrode, counter electrode, nitrogen bubbler, and thermocouple well. Butyronitrile (Aldrich or Eastman reagent grade) was stirred at 75 °C over 11 g of potassium permanganate and 7.7 g of sodium carbonate per liter for 16 h and distilled through a 24 in. vigreaux column at 15 mm of nitrogen pressure. After repetition of this procedure, the first and last quarter of the distillate were discarded and the middle portion stored in a brown bottle over alumina (activated at 350 °C for 24 h). The final purification step was distillation through a Nester and Faust Teflon spinning band column at 15 mm of nitrogen pressure. The supporting electrolyte was 0.1 M tetrabutylammonium perchlorate (Aldrich) which had been recrystallized from 50% ethanol and dried in a vacuum dessicator at 0.1 mm for at least 24 h. A $1-2 \times 10^{-3}$ M solution of hydrazine was employed, and about 10 ml of solution was required to fill our cell.

Cyclic voltammograms at 50–250 mV/s scan rates were recorded on a Hewlett-Packard 7004B XY recorder and faster scan rates on a Tecktronix 564B storage oscilloscope.

Acknowledgments. We thank the National Science Foundation (Grants CHE75-04930, MPS74-19688) and the Wisconsin Alumni Research Foundation for partial financial support of this work.

References and Notes

(1) For 1, see S. F. Nelsen, L. Echegoyen, and D. H. Evans, *J. Am. Chem. Soc.*, **97**, 3530 (1975).
(2) S. F. Nelsen, V. E. Peacock, and G. R. Weisman, *J. Am. Chem. Soc.*, **98**, 5269 (1976).
(3) R. P. Van Duyne and C. N. Reilley, *Anal. Chem.*, **44**, 142 (1972).
(4) (a) S. F. Nelsen and G. R. Weisman, *J. Am. Chem. Soc.*, **98**, 3281 (1976); (b) *ibid.*, **98**, 7007 (1976).
(5) S. F. Nelsen and J. M. Buschek, *J. Am. Chem. Soc.*, **98**, 6787 (1974), and references therein
(6) S. F. Nelsen, G. R. Weisman, P. J. Hintz, D. Olp, and M. R. Fahey, *J. Am. Chem. Soc.*, **96**, 2916 (1974).
(7) M. S. Shuman and I. Shain, *Anal. Chem.*, **41**, 1818 (1969).
(8) S. Feldberg in "Electroanalytical Chemistry", Vol. 3, A. J. Bard, Ed., Marcel Dekker, New York, N.Y., 1969, pp 199–295.
(9) I. Ruzic and S. Feldberg, *J. Electroanal. Chem.*, **50**, 153 (1974).
(10) D. H. Evans, unpublished calculations, University of Wisconsin, 1973.
(11) R. S. Nicholson and I. Shain, *Anal. Chem.*, **36**, 706 (1964).
(12) R. S. Nicholson and I. Shain, unpublished calculations, University of Wisconsin, 1963.
(13) D. H. Evans, *J. Phys. Chem.*, **76**, 1160 (1972).
(14) R. S. Nicholson, *Anal. Chem.*, **37**, 667 (1965).
(15) R. S. Nicholson, *Anal. Chem.*, **37**, 1351 (1965).
(16) H. W. VandenBorn and D. H. Evans, *Anal. Chem.*, **46**, 643 (1974).
(17) J. E. Anderson, *J. Am. Chem. Soc.*, **91**, 6374 (1969).
(18) F. A. L. Anet and M. Z. Haq, *J. Am. Chem. Soc.*, **87**, 3147 (1965).
(19) F. A. L. Anet and A. J. R. Bourn, *J. Am. Chem. Soc.*, **89**, 760 (1967).